FRESH™ 3D bioprinted cardiac tissue, a bioengineered platform for *in vitro* pharmacology

View Online   Export Citation   CrossMark

Samuel Finkel,[1] Shannon Sweet,[1] Tyler Locke,[1] Sydney Smith,[1] Zhefan Wang,[1] Christopher Sandini,[1] John Imredy,[2] Yufang He,[3] Marc Durante,[3] Armando Lagrutta,[2] Adam Feinberg,[1,4,5] and Andrew Lee[1,a]

AFFILIATIONS

[1]FluidForm, Inc., Waltham, Massachusetts 02451, USA
[2]In Vitro Safety Pharmacology, Genetic and Cellular Toxicology, Merck & Co. Inc., Rahway, New Jersey 07065, USA
[3]Division of Technology, Infrastructure, Operations and Experience, Merck & Co. Inc., Rahway, New Jersey 07065, USA
[4]Department of Biomedical Engineering, Carnegie Mellon University, Pittsburgh, Pennsylvania 15213, USA
[5]Department of Materials Science and Engineering, Carnegie Mellon University, Pittsburgh, Pennsylvania 15213, USA

[a]Author to whom correspondence should be addressed: andrew@fluidform3d.com

ABSTRACT

There is critical need for a predictive model of human cardiac physiology in drug development to assess compound effects on human tissues. *In vitro* two-dimensional monolayer cultures of cardiomyocytes provide biochemical and cellular readouts, and *in vivo* animal models provide information on systemic cardiovascular response. However, there remains a significant gap in these models due to their incomplete recapitulation of adult human cardiovascular physiology. Recent efforts in developing *in vitro* models from engineered heart tissues have demonstrated potential for bridging this gap using human induced pluripotent stem cell-derived cardiomyocytes (hiPSC-CMs) in three-dimensional tissue structure. Here, we advance this paradigm by implementing FRESH™ 3D bioprinting to build human cardiac tissues in a medium throughput, well-plate format with controlled tissue architecture, tailored cellular composition, and native-like physiological function, specifically in its drug response. We combined hiPSC-CMs, endothelial cells, and fibroblasts in a cellular bioink and FRESH™ 3D bioprinted this mixture in the format of a thin tissue strip stabilized on a tissue fixture. We show that cardiac tissues could be fabricated directly in a 24-well plate format were composed of dense and highly aligned hiPSC-CMs at >600 million cells/mL and, within 14 days, demonstrated reproducible calcium transients and a fast conduction velocity of ~16 cm/s. Interrogation of these cardiac tissues with the β-adrenergic receptor agonist isoproterenol showed responses consistent with positive chronotropy and inotropy. Treatment with calcium channel blocker verapamil demonstrated responses expected of hiPSC-CM derived cardiac tissues. These results confirm that FRESH™ 3D bioprinted cardiac tissues represent an *in vitro* platform that provides data on human physiological response.

INTRODUCTION

Cardiovascular disease is a major burden on the global healthcare system and the leading cause of death worldwide.[1] While there are a range of highly effective cardiovascular drugs for treating high blood pressure, cholesterol, and acute heart failure, there have been very few new drugs approved for treating chronic arrhythmogenic, contractile, or cardiometabolic diseases of the myocardium itself.[2] Indeed, the number of approved cardiac compounds have stagnated due to high failure rates in clinical trials, leading to the pharmaceutical industry decreasing investment in the development of new cardiac assets,

despite the well-recognized healthcare burden.[3,4] These low approval rates and lack of drug pipelines addressing cardiovascular indications can be attributed to the complexity of cardiac physiology and the associated difficulty in appropriately assessing cardiac drug safety and efficacy prior to preclinical and clinical trials.[5–7] Differences between human and animal cardiac physiology limit the quality of insights drawn from preclinical studies, further hampering development efforts.[3,8,9] The FDA Modernization Act 2.0 passed by the United States Congress in 2022[10] seeks to remove preclinical animal data from the regulatory approval process before a drug enters human clinical

trials by using predictive *in vitro* models; however, for heart disease, these models still need to be improved before they are viable for this application.

The development of human induced pluripotent stem cell-derived cardiomyocytes (hiPSC-CMs) has made *in vitro* culture a promising approach to evaluate drug safety and efficacy, with the potential to replace animal models as the key tool for insight generation in lead optimization prior to human clinical studies.[11–17] Over the past decade, two-dimensional (2D) hiPSC-CM monolayer cultures have been adopted with the promise of more physiologically relevant readouts and straightforward integration into conventional well-plate workflows in high-throughput screening.[18] Despite their rapid adoption, growing evidence indicates 2D monolayer hiPSC-CM systems do not fully recapitulate the three-dimensional (3D) structure and function of the adult heart, limiting their value primarily to biochemical and cellular-scale assays.[19] Cardiac spheroids and organoids provide an ability to place hiPSC-CMs in a 3D structure, and this clearly provides some advantages; however, the structure and function still recapitulates the embryonic state at best.[20] Engineered heart tissues (EHTs) have been developed to better recreate the 3D structure and function of the heart at the tissue and organ scale, leading to more physiologically data-rich assays.[21–30] Current 3D fabrication approaches for hiPSC-CMs through molding of cell-laden hydrogels, seeding on fiber-based scaffolds, and 3D bioprinting have been effective in creating contractile cardiac tissues in a dish. However, there remains a wide range of hiPSC-CM maturation states, tissue structural organization, electrophysiology, contractility, and drug responses.

Here, we demonstrate that freeform reversible embedding of suspended hydrogels (FRESH™) 3D bioprinting can be used to fabricate EHTs in a multi-well plate format, taking advantage of the parametric design and robotic control of the additive manufacturing process to control tissue composition, architecture, and reproducibility. FRESH™ 3D bioprinting works by extruding cell-laden bioinks within a gelatin microparticle support bath that provides mechanical support to the bioink while it gels and then can be nondestructively removed by melting at 37 °C.[31] We have previously demonstrated that FRESH™ 3D bioprinting can be used to engineer cardiac tissues in a range of complex 3D structures such as ventricle-like constructs and heart tubes with advanced functionality.[29,30] To expand upon this, we created a process that enables EHTs to be FRESH™ 3D printed around custom-designed tissue fixtures within 24-well plates and then performed structural, functional, and pharmacologic assays to demonstrate platform capabilities. Importantly, engineered cardiac tissues have high hiPSC-CM density, uniaxial aligned cells, and exhibit spontaneous contractility. In this report, we establish manufacturing reproducibility, multi-well plate compatibility, and pharmacological response consistent with expected chronotropy and inotropy, which provides a foundation for future applications in drug discovery.
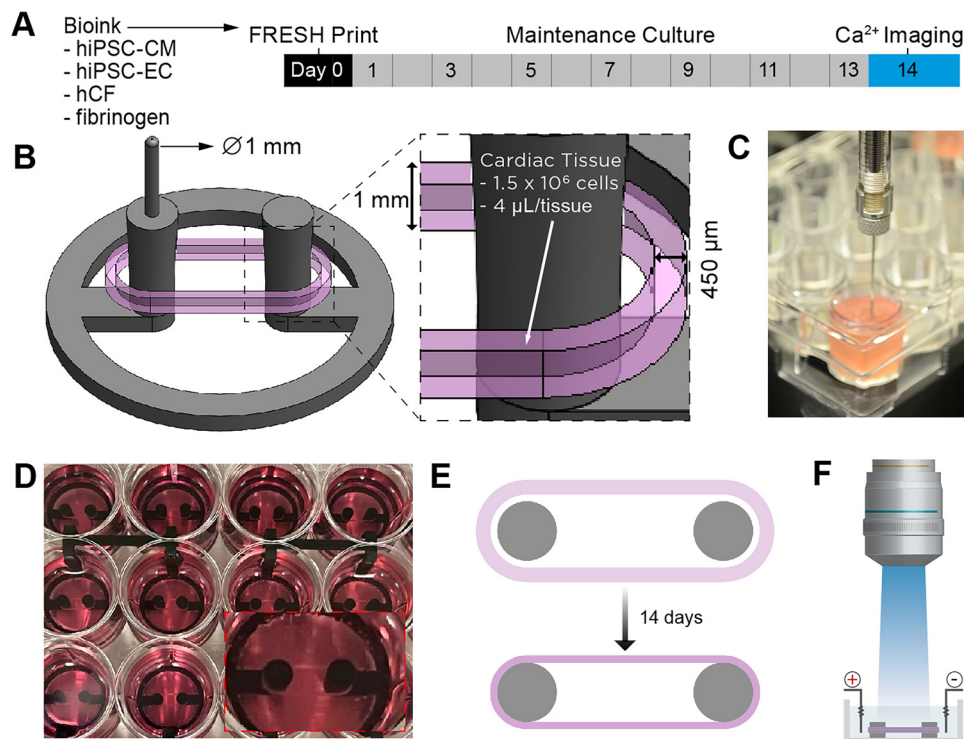

FIG. 1. Fabricating FRESH™ printed cardiac tissue strips in a 24-well plate format. (a) Timeline of the fabrication process from FRESH™ printing at day 0 to calcium imaging at day 14. (b) Schematic of the cardiac tissue (pink) designed to be FRESH™ printed around support posts (gray). (c) Image of FRESH™ printing using a cell-laden bioink, printing into a single well. (d) Top-down view of cardiac tissues in each well showing the 24-well plate format; inset shows a cardiac tissue in a single well. (e) Schematic of cardiac tissue compaction around support posts over time in culture. (f) Schematic of the cardiac tissue used for high-resolution, high-speed calcium imaging.

RESULTS

Engineering of cardiac tissues

FRESH™ 3D bioprinted cardiac tissues were designed and fabricated with several key attributes in mind, specifically, multi-well plate compatibility, biomanufacturing speed and reproducibility, rapid stabilization of tissue function, compatibility with high-quality calcium imaging, and both chronotropic and inotropic response to isoproterenol and verapamil. Cardiac tissues were FRESH™ printed using a cell-laden bioink prepared with cells directly from cryopreservation, composed of 75% hiPSC-CMs, 10% hiPSC-ECs, and 15% primary adult ventricular human cardiac fibroblasts (hCFs). This was followed by culture for 14 days to reach a stable state [Fig. 1(a)]. The design consisted of a strip of cardiac tissue 450 μm wide and 1 mm high printed in an obround shape around a fixture with two support posts [Fig. 1 (b)]. Using a cell bioink concentration of 320×10^6 cells/ml, we printed 1.3×10^6 cells in 4 μl volume of bioink per tissue at the time the cardiac tissue was fabricated. This cell density is approximately an order-of-magnitude greater than that typically used in 3D

bioprinting.[34,35] The support fixtures were embedded in LifeSupport™ within each well, and the needle tip of the extruder was aligned to the reference guide for each fixture, which allowed for accurate and precise extrusion and reproducible fabrication of each tissue [Fig. 1(c)]. Through the robotic control provided by the 3D bioprinter, manufacturing of a full 24-well plate of cardiac tissues was completed in under 30 min [Fig. 1(d)]. After printing, the cardiac tissues were cultured for 14 days during which the hCFs actively compacted the tissue around the two posts of the support fixture, resulting in dense and highly aligned hiPSC-CMs [Fig. 1(e)]. This design also enabled high resolution, high-speed calcium imaging, from which to assess calcium transient and action potential propagation behavior [Fig. 1(f)].

Structural characterization of cardiac tissues

Following printing, the cardiac tissues underwent a 14-day culture process during which tissues compacted and aligned. Within the first hour post-printing, the cardiac tissues began to compact around the pillars of the fixture [Fig. 2(a)]. On day 1 post-printing, the cardiac
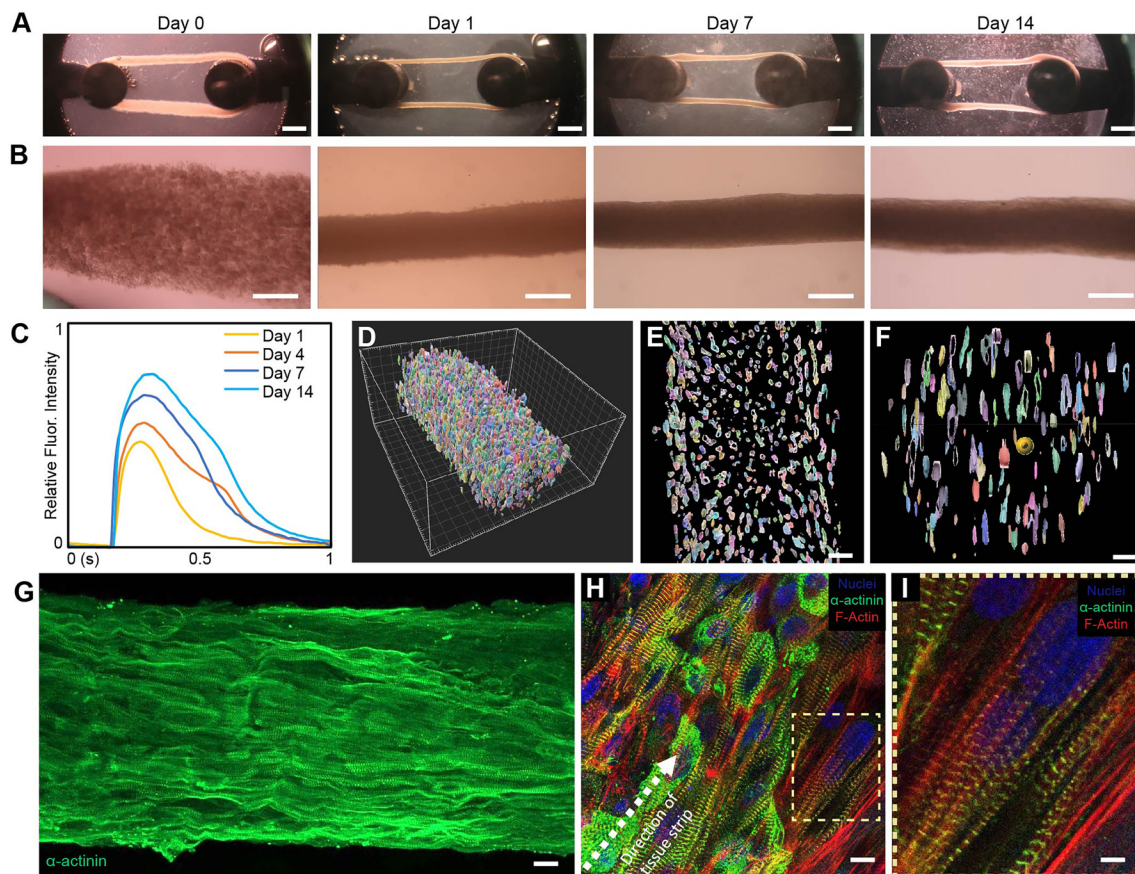

FIG. 2. Structural characterization of the FRESH™ printed cardiac tissue. (a) Brightfield images of cardiac tissue strips throughout time in culture show compaction and remodeling of tissue strip over time. Scale bars are 1 mm. (b) Higher magnification images of tissues during culture. Scale bars are 100 μm. (c) Calcium transients of cardiac tissues at different time points in culture demonstrating maximum amplitude at 14 days. (d) 3D segmented and color-coded Z-stack of nuclei reveal high cell density throughout the tissue, including in (e) longitudinal and (f) transverse cross sections. Scale bars are 20 μm. (g) Fluorescent image showing uniaxial alignment of sarcomeres with high cell density. Scale bar is 10 μm. (H) High magnification imaging of cardiomyocytes show alignment along length of tissue and (i) well-organized sarcomeric structures. Tissues are stained for nuclei (blue), a-actinin (green), and F-actin (red.) Scale bars are 20 μm for (h) and 5 μm for (i).

tissue had compacted around the fixturing posts further, and rapidly contracting clusters of hiPSC-CMs were dispersed throughout the tissue. By day 7, the cardiac tissues had compacted completely and begun beating synchronously. An additional 7 days of culture, for 14 days total, was required for the cardiac tissue to reach its fully stable shape. Of all the tissues printed, 80% survived to 14 days in culture (n = 171, Table S1, Fig. S1). Tissues imaged at day 0 of culture showed slight geometric variability because of the tissue release process from the support bath; however, following compaction at day 1, those differences were minimal (Fig. S2). After 14 days of culture, variability between wells in a plate and between print batches was also minimal. Quantitative measurement of tissue width at day 0 and day 14 corroborated the findings of reproducibility as determined by tissue width (n = 33, Fig. S3). At higher magnification, the change in cardiac tissue morphology with time could be seen as the compaction and densification of the tissue, reaching a final diameter on the order of ~300 μm on day 14 [Fig. 2(b)]. Several tissues were cultured for >80 days, throughout which tissue morphology and beat rate remained similar to day 14 tissues. At day 14, the cardiac tissue also reached a maximum in the calcium transient amplitude, which remained consistent through 28 days in culture [Fig. 2(c)]. Whole-mount 3D confocal imaging of the cardiac tissue on day 14 stained for cell nuclei demonstrated the high cell density that was achieved [Fig. 2(d) and Video S1]. Cross sections of the tissue strip in the longitudinal and transverse directions confirmed that cell density was consistent through the entire thickness and that cell viability was maintained [Figs. 2(e) and 2(f)]. Calculation of nuclei density shows that tissues printed with an initial bioink concentration of ~320 × 10⁶ cells/ml further compacted to day 14 tissues with cellular density of >600 × 10⁶ cells/cm³. This appears to be the highest cell density reported in the literature for an engineered cardiac tissue and is on par with the density reported for neonatal human myocardium.[36] Immunofluorescent staining of sarcomeric α-actinin confirmed that the cardiac tissue contained highly aligned cardiomyocytes in the longitudinal direction of tension from the printing and compaction process [Figs. 2(g) and 2(h)]. Further assessment of cardiac subcellular structure deeper within the tissue strip showed well-organized sarcomeres perpendicular to the direction of cellular alignment [Fig. 2(l)].

Electrophysiology of FRESH™ printed cardiac tissues

The electrophysiology of the FRESH™ printed cardiac tissues was assessed using high-speed and high-resolution calcium imaging. Whole tissue recording of calcium dynamics at day 14 revealed presence of a contractile syncytium with visually observable calcium wave propagation [Fig. 3(a) and Video S2]. Of the 80 tissues that were calcium imaged, 94% had stable contraction with a beat rate between 30 and 100 bpm [Table S1 and Figs. S4(a) and S4(b)]. High magnification imaging of representative regions of interest (ROIs) along the length of tissue displayed comparable calcium trace morphology, indicating the formation of a uniform cardiac tissue substrate with consistent calcium transient properties by day 14 [Fig. 3(b) and Video S3]. Conduction velocity in the longitudinal direction of the tissue strips was measured to be 15.98 ± 3.47 cm/s [Fig. 3(c)], comparable to the highest values reported from other engineered heart tissues cultured under electrical stimulation conditions designed to drive maturation.[37] Consistent with human adult sinus rhythm, cardiac tissues developed an automaticity-driven spontaneous beat rate of 60.7 ± 29.7 bpm. When paced under electrical field stimulation, FRESH™ printed cardiac tissues responded as a syncytium and were fully captured at 2 and 3 Hz. Pacing frequencies at or below 1 Hz led to the rise of intermittent contractions between stimulation pulses because of the higher spontaneous beat rate of some tissues [Fig. 3(d)].
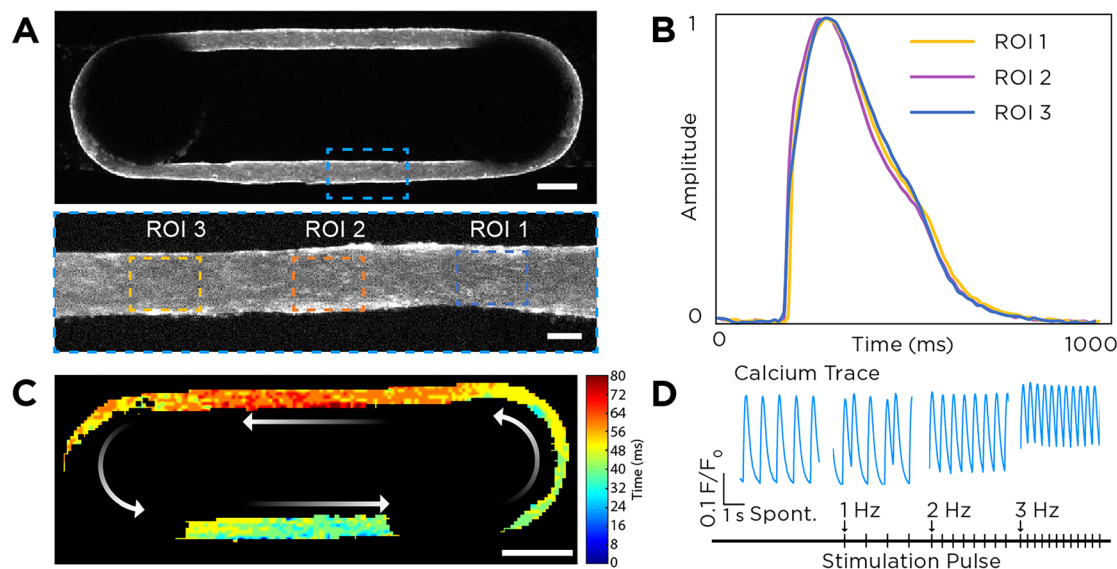

FIG. 3. Characterization of FRESH™ printed cardiac tissue calcium handling. (a) Top-down views of a representative cardiac tissue stained with calcium-sensitive dye showing uniform cell distribution. Scale bars are 750 μm (top) and 150 μm (bottom). (b) Plot of calcium transients from the three ROIs in panel (a) showing uniform calcium waveform morphology. (c) Calcium optical mapping of the whole tissue enables observation of the spontaneously propagating action potential and calculation of the conduction velocity. Scale bar is 1 mm. (d) Representative calcium transient for cardiac tissues undergoing spontaneous and electrically stimulated contractions at 1, 2, and 3 Hz.

FRESH™ printed cardiac tissues display drug responses consistent with expected chronotropy and inotropy

To investigate the functional drug response of FRESH™ printed cardiac tissue strips, we assessed tissue calcium response to the tool compounds isoproterenol and verapamil. When treated with a saturating level of isoproterenol at 2.5 μM, the FRESH™ printed cardiac tissues responded with ~40% increase in beat frequency and ~35% increase in calcium amplitude when compared to untreated baseline [Fig. 4(a) and Video S4]. A decrease in calcium cycling time was also

observed, marked by both a decrease in calcium transient duration as well as faster relaxation kinetics [Fig. 4(b)]. This response was observed consistently across multiple batches of tissues, where 85% of all tissues measured responded to drug treatment (Table S1). To understand the robustness of this response, we evaluated the isoproterenol-treated calcium dynamics in cardiac tissues FRESH™ printed from print batches using the same cell compositions from an additional commercial hiPSC-CM cell line lot [Fig. 4(c)], as well as in cardiac tissues FRESH™ printed with different compositions of cardiomyocytes,
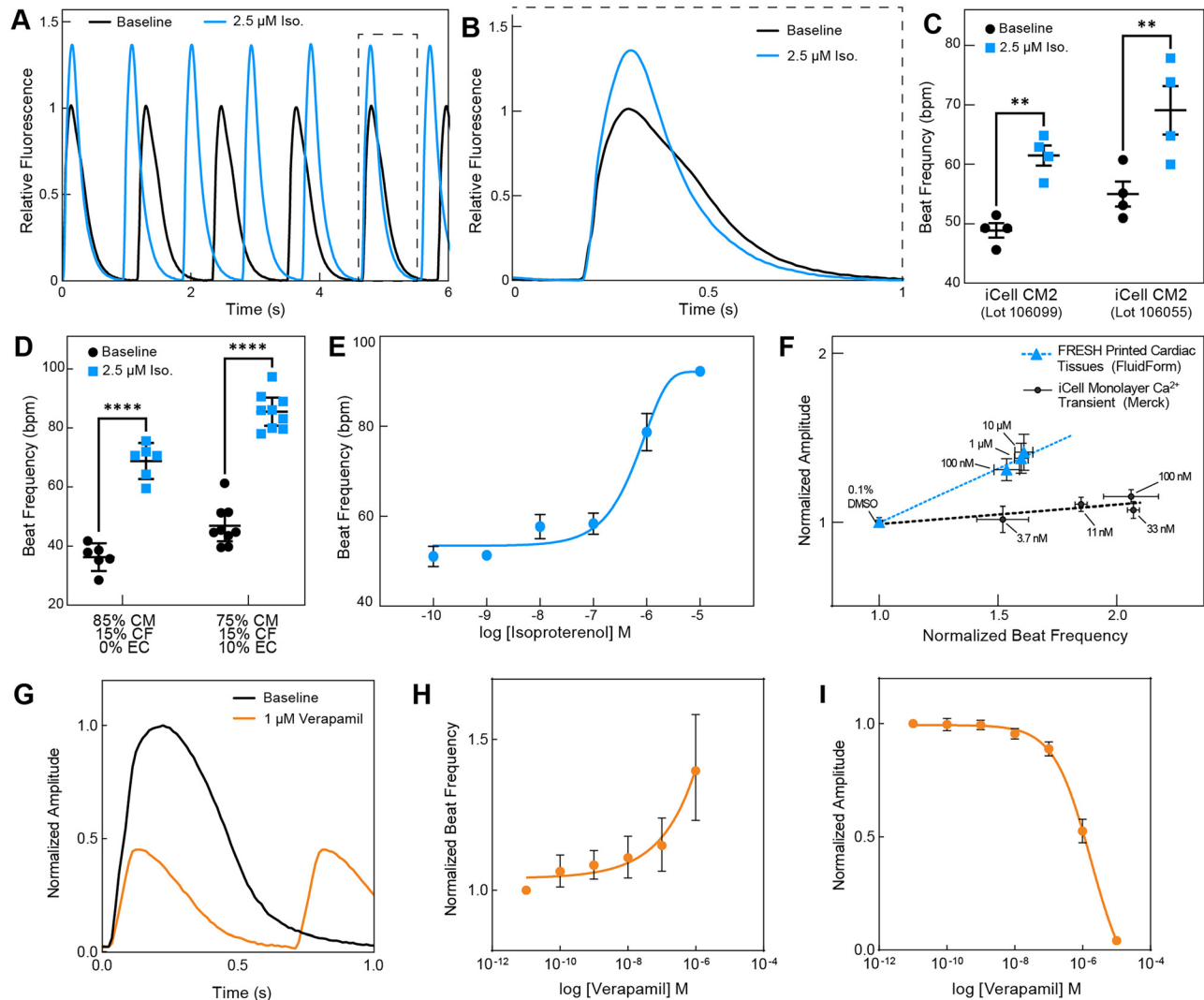

FIG. 4. FRESH™ printed cardiac tissues exhibit positive chronotropic and inotropic responses to β-adrenergic receptor agonist isoproterenol L-type calcium channel antagonist verapamil. (a) Representative calcium transients from FRESH™ printed cardiac tissue at baseline and exposure to 2.5 μM of isoproterenol. (b) Direct comparison of a single calcium transient for baseline and isoproterenol treated (2.5 μM) shows the characteristic 30%–40% increase in peak amplitude. (c) Spontaneous beat frequency in response to 2.5 μM of isoproterenol reveals comparable chronotropic response in cardiac tissues FRESH™ printed with different commercially available hiPSC-CM lots. (d) Spontaneous beat frequency in response to 2.5 μM of isoproterenol reveals comparable chronotropic response in cardiac tissues FRESH™ printed with different cellular compositions, either with two cell types (hiPSC-CMs and hCFs) or with three cell types (hiPSC-CMs, hiPSC-ECs, and hCFs). (e) Dose response curve of cardiac tissue beat frequency as a function of isoproterenol concentration showing chronotropic response (n = 3). (f) Dose response curves of normalized calcium transient amplitude as a function of normalized beat rate for isoproterenol-treated hiPSC-CM 2D monolayers as compared to FRESH™ 3D printed cardiac tissues (n = 4 for FRESH™ printed tissues and n = 9 wells for iCell monolayers). (g) Direct comparison of a single calcium transient for baseline and verapamil treated (1 μM). (h) Beat frequency and (I) calcium amplitude response to verapamil dosing.

endothelial cells, and cardiac fibroblasts [Fig. 4(d)]. Results show that in response to isoproterenol, cardiac tissues fabricated from a different hiPSC-CM lot maintained positive chronotropy, and cardiac tissues fabricated with hiPSC-CMs and hCFs but without hiPSC-ECs also maintained a positive chronotropy. Finally, chronotropic dose response to isoproterenol in terms of beat frequency followed the expected curve with the transition from sub-threshold to saturating dose and an EC50 of 1 μM [Fig. 4(e) and Video S5]. The FRESH^{TM} printed cardiac tissues also showed a positive relationship between beat rate and calcium amplitude response as a function of isoproterenol dose [Fig. 4(f)]. This positive relationship is absent in iCell hiPSC-CMs cultured in 2D monolayers, which show a positive chronotropic response but minimal calcium amplitude response as a function of isoproterenol dose. Thus, the FRESH^{TM} printed cardiac tissues are able to reproduce responses consistent with the chronotropic and inotropic response of isoproterenol. When treated with a saturating level of verapamil at 1 μM, we saw a marked decrease in calcium amplitude as well as an increase in beat frequency [Fig. 4(g)]. Dose response experiments with verapamil show a dose-dependent effect on positive chronotropy and decrease in calcium amplitude [Figs. 4(h) and 4(1)]. This decrease in calcium amplitude was associated with a visually observable reduction in contractile activity, consistent with negative inotropy.

DISCUSSION

This study demonstrates well-plate-based manufacturing of cardiac tissues for use in interrogating drug effects on human tissues. Key to this is the FRESH^{TM} 3D bioprinting process, which enables the use of high-density cell bioinks of $>320 \times 10^6$ cells/ml that remodel into cardiac tissues with densities of $>600 \times 10^6$ cells/ml and uniaxially aligned hiPSC-CMs. Except for other work making use of FRESH^{TM} for 3D bioprinting cardiac tissue, we are not aware of any other biofabrication or tissue engineering approaches that can achieve comparable cell densities and uniaxial alignment.[30] We also used commercially available hiPSC-CMs, hiPSC-ECs, and hCFs from cryopreservation that were directly combined into the bioink for bioprinting. Not only did this enable us to demonstrate our platform with one of the most widely used hiPSC-CM cell lines in academic and industry research, but it also decoupled the timeline of the cell culture process from the bioprinting process. Overall, this builds off of previous work, leveraging FRESH^{TM} bioprinting for the fabrication of functional cardiac tissues[30] together with other studies working toward utilization of engineered heart tissue for *in vitro* models in drug discovery.[38] With our platform, we were able to expand upon this previous work by creating a tissue strip designed to be reproducibly manufactured in a multi-well plate format (Figs. 1 and S1–S5), form cardiac tissue with high density and alignment characteristic of human myocardium (Fig. 2), achieve high conduction velocity (Fig. 3), and demonstrate beat rate and calcium amplitude responses consistent with expected chronotropic and inotropic responses to a β adrenoceptor agonist and a L-type calcium channel blocker (Fig. 4).

The FRESH^{TM} bioprinting technology allowed for the creation of engineered cardiac tissues that overcome several limitations of other cardiac tissue models. Most engineered cardiac tissues are fabricated using cardiomyocytes mixed within a hydrogel matrix at a concentration of $1–30 \times 10^6$ cells/ml.[11,22,25,39–41] This relatively low cell concentration is typically driven by the need to have enough hydrogel to achieve adequate mechanical properties when gelled to hold the cardiac tissue together. Here, we demonstrated the ability to process and handle a significantly higher cell concentration bioink (of $\sim 320 \times 10^6$ cells/ml) through use of FRESH^{TM} printing within a support bath, allowing us to fabricate tissues at cardiomyocyte densities on par with native myocardium.[36] We hypothesize that this native-like cell density in FRESH^{TM} printed cardiac tissues facilitates a high degree of cardiomyocyte alignment and electromechanical coupling, and in conjunction with the high aspect ratio of the cardiac tissue strip helped drive cardiomyocyte anisotropy along the longitudinal axis, resulting in the observed conduction velocity of ~ 16 cm/s, close to the adult physiologic range of $\sim 40–60$ cm/s.[42,43] While this native-like cell density would suggest steeper metabolic demands and higher nutrient and oxygen requirements, our data indicated that our approach to bioprint thin cardiac microtissues ($<300 \mu$m when fully stabilized) allows us to avoid hypoxic scenarios. Cardiac tissues of similar dimensions reported in the literature have shown histological cross sections of tissues that showed absence of cell bodies at the tissue core,[44–46] indicating cell death and breakdown of the cellular structure and contents, which we do not see in our tissues. We did observe a difference in cell morphology at the surface of the tissue (highly aligned) and toward the center of the tissue (less dense myofibrils). It is unclear why this morphology difference occurs, and future studies are needed to elucidate the possible mechanisms in demands on oxygen or nutrient gradients, mechanical tension differences between the surface and interior of the tissue, self-segregation of different cell types, or a combination of multiple factors. In addition to improving cardiac tissue structural maturity, we also hypothesize that the native-like cellular density enabled observed isoproterenol responses consistent with chronotropy and inotropy [Figs. 4(e) and 4(f)]. This response to β adrenoceptor agonist treatment has been demonstrated in other engineered heart tissues, usually after the cardiac tissues have undergone frequency-ramped electrical pacing regimen.[37,47] Here, we were able to show adrenergic responsiveness in a 14-day culture and drug testing cycle without the use of supraphysiological pacing regimen, allowing for quick iterations on experimental design and functional drug response assessments.

Furthermore, FRESH^{TM} printing enabled a design-for-purpose engineering approach, which we leveraged in this study to prioritize design for well-plate compatibility, manufacturing reproducibility, small tissue dimensions, and ease of calcium imaging and analysis. Our data showed that using this robotic fabrication approach, we are able to achieve high print and release success rates, specify compacted tissue structure and survival through culture, and maintain functional response across tissues and batches. Calcium amplitude response was relatively consistent across prints and batches (Fig. S5), indicating a well-established beta-adrenergic signaling cascade within our tissues after 14 days of culture. We did observe batch to batch variations in chronotropic response to isoproterenol, which we hypothesize is the result of the inherent immaturity of iPSC-CMs utilized in the studies, leading to unpredictable spontaneous depolarizations. Future work will focus on further automation of tissue release, media exchange, and electrical stimulation during culture; all of which should contribute to higher tissue survival rate and more consistent functional response to pharmacological compounds.

Overall, we were successful in engineering contractile cardiac tissues; however, it is important to note that these tissues do not fully recapitulate adult cardiac function. First, the tissues that we engineered displayed automaticity, a property of fetal cardiac tissues, which is

common in cardiac tissues engineered from hiPSC-CMs.[25,48–52] Second, our tissues exhibited a flat force–frequency relationship (as quantified by calcium transients), which is different from the positive force–frequency relationship found in adult human myocardium.[53,54] This behavior, together with an absence of post-rest potentiation, suggests immature sarcoplasmic reticulum function compared to the adult heart.[55] Third, while our tissues responded to isoproterenol similar to adult myocardium with responses consistent with positive chronotropy and inotropy, additional investigation is needed to determine whether this is due to an increase in the I_{Ca} caused by β-adrenergic receptor activation followed by phosphorylation of the L-type Ca^{2+} channel $Ca_V1.2$, or if it is a result of phosphorylation of phospholamban and an increased rate of sarcoplasmic reticulum Ca^{2+} loading.[56–58] Fourth, while our observed responses to verapamil is consistent with what has been reported in the literature (positive chronotropy and negative inotropy) for engineered heart tissues generated from human iPSC-CMs,[59,60] the positive chronotropic response is different from the negative chronotropy reported in adult human cardiac tissues. This difference suggests relative immaturity of calcium handling in hiPSC-CMs utilized in this study compared to that of adult cardiomyocytes. Further baseline characterization of calcium handling functional maturity is required in our cardiac tissues. Additional implementation of maturation strategies affecting calcium release and reuptake capacity[47] would likely yield cardiac tissues that are responsive to the chronotropic and inotropic effects of calcium blockers. Finally, we did not perform ultrastructural analysis to assess whether the hiPSC-CMs contained structural components of mature heart tissue such as the presence of T-tubules. In summary, while we have achieved a number of advances with this platform, there is clearly room for further improvement as the entire field using hiPSC-CMs works toward fully recapitulating the physiology of adult myocardium.[16]

Future work will focus on confirming the capabilities of this platform for *in vitro* toxicology and pharmacology, both to develop novel disease models for drug discovery[16,17] as well as to ultimately replace pre-clinical animal testing as outlined in the FDA Modernization Act 2.0 passed by the United States Congress in 2022.[10] This includes working to improve upon multiple factors that can drive functional maturation, such as the implementation of a dynamic loading regime that can reproduce both preload and afterload. The dynamic engineered heart tissue (dyn-EHT) developed by Bliley *et al.* demonstrates the importance of preload in driving structural and functional maturation of cardiac tissue as compared to most EHT systems that only generate afterload.[29] This dyn-EHT application of preload has also been shown to be critical in driving the emergence of disease phenotypes linked to genetic mutations, such as in arrhythmogenic cardiomyopathy and dilated cardiomyopathy.[29,61] Other factors to implement that can drive cardiac tissue maturation include electrical stimulation during culture,[62] biochemical stimulation such as triiodo-L-thyronine (T3) hormone,[46] and fatty acid metabolism.[63–66] Additional functional readouts are also needed, including contractile force and voltage mapping to quantify the action potential. Cardiac tissues engineered to recapitulate tissue and organ-scale disease states will represent significant next steps to provide clinically translatable data. This includes genetic-based cardiomyopathies (e.g., dilated, hypertrophic, arrhythmogenic) that can be recreated using patient-derived and/or gene-edited hiPSC-CM lines with monogenic or polygenic mutations.[16]

Other forms of heart disease associated with aging also have the potential to be replicated; in the case of FRESH™ 3D bioprinting, the reported ability to print collagen[30] could be used to develop late-stage cardiac fibrosis models through multi-material printing and parametric design based on histology.[67] The tissue design can also be modified to model arrhythmias where irregular electrical signal initiation and propagation can be controlled through multi-material deposition to engineer cardiac substrate heterogeneity in order to potentiate irregularly propagating action potentials. Taking all of these examples together, it is clear that there are a wide range of approaches to improve engineered cardiac tissue function, and our FRESH™ 3D bioprinted platform has the potential to incorporate many of them.

METHODS

Multi-well plate design and fabrication

To create an *in vitro* array of engineered cardiac tissues, FRESH™ printing was performed within specially designed 24-well plates with integrated tissue fixtures. The tissue fixtures were designed using SolidWorks (Dassault Systemes) and 3D printed on a Formlabs Form 3B printer (Formlabs) using BioMed Clear (RS-F2-BMCL-01, Formlabs) or BioMed Black resin (RS-F2-BMBL-01, Formlabs). Following printing, the fixtures were cured at $70\,^{\circ}C$ for 60 min, post-processed to remove support material from printing, washed in an isopropanol bath for 15 min, airdried, and then sterilized by autoclaving. The tissue fixtures were then placed within each well of a cell-culture grade 24-well plate (229124, CellTreat).

FRESH support bath preparation

All FRESH™ printing was performed with LifeSupport™, a gelatin microparticle support material prepared according to manufacturer's directions. Briefly, 1 g LifeSupport™ (FluidForm) was rehydrated in cold ($4\,^{\circ}C$) DMEM/F-12 (11320033, Gibco). Rehydrated LifeSupport™ was centrifuged, supernatant was removed from the tube, and the compacted LifeSupport™ was resuspended in DMEM/F-12 containing $1\times$ P/S (P0781, Sigma Aldrich) and 10 U thrombin (91–030, BioPharm Laboratories). Thrombin-supplemented LifeSupport™ was centrifuged again, and the supernatant was aspirated. A 14G sterile needle was used to transfer the compacted LifeSupport™ into designated wells of a 24-well plate.

Cell-laden bioink preparation

The cell-laden bioink was prepared as a high-density combination of three cardiac cell types: specifically, hiPSC-CMs (iCell Cardiomyocytes[2] 01434, R1017 Fujifilm Cellular Dynamics), hiPSC-ECs (iCell Endothelial Cells 01434, R1022 Fujifilm Cellular Dynamics), and primary adult ventricular cardiac fibroblasts (C-12375, PromoCell). The primary adult ventricular cardiac fibroblasts (hCFs) were purchased at low passage, expanded in culture to 70% confluency in fibroblast growth medium (C-23130, PromoCell) and cryopreserved for later use. Endothelial cell concentrations were determined based on a recent report.[32] At the time of bioink preparation, all cells were removed from liquid nitrogen storage, thawed, and transferred to media according to the manufacturer's instructions. Following thaw, the hiPSC-CMs, hCFs, and hiPSC-ECs were mixed at the desired cell composition and centrifuged at $200\times$ g for 7 min. The cells were resuspended in 20 mg/ml fibrinogen (9001–32-5, Millipore

Sigma) and DMEM/F-12 medium and transferred into a sterile gastight syringe (81230, Hamilton). The gastight syringe was capped, fitted into a custom 3D printed syringe centrifuge adapter, and centrifuged at 200× g for 7 min. The supernatant was aspirated from the syringe, and the syringe was fitted with a blunt tip needle, ready for printing. All syringes, needles, adapters, and syringe accessories were sterilized in the autoclave prior to use.

Design and FRESH[TM] 3D bioprinting of cardiac tissues

The cardiac tissue was printed within the wells of a 24-well plate with an obround shape suspended between two support posts. The overall dimensions of the cardiac tissue construct as printed were 10 mm length, 2.5 mm width, and 1 mm height, with the tissue strip itself printed with a height of 1 mm and a width of 450 μm. The cardiac tissue was designed in computer-aided design (CAD) software, exported in the STL file format, and then sliced into G-code with a filament diameter of 450 μm and a print speed of 5 mm/s. FRESH[TM] 3D bioprinting of the cardiac tissue was performed under sterile condition in a biosafety cabinet on a custom-built extrusion 3D bioprinter equipped with a Replistruder 4 syringe pump extruder.[33] For printing, the syringe containing the cell bioink was mounted on the printer, and the 24-well plate containing the tissue fixtures and LifeSupport[TM] in each well was positioned on the build platform. For each tissue, the needle of the printer was aligned with a thin calibration post located on each fixture. This calibration post serves as a reference origin for each print, the alignment to which ensures accurate placement of the tissue around the fixture posts without interference by the fixture to needle travel. After printing, the multi-well plate was transferred to a 37 °C incubator for 30 min to melt the LifeSupport[TM] and release the cardiac tissues, and then rinsed with DMEM/F12 to remove excess gelatin in the well. The media in each well was then replaced with 1× P/S supplemented maintenance medium made from 80% cardiomyocyte medium (M1003, Fujifilm Cellular Dynamics), 20% endothelial cell growth medium (C-22010, PromoCell). Cardiac tissues were typically maintained for 2 weeks. The maintenance medium was replenished every 2 days.

Calcium imaging and analysis

Calcium imaging was performed to assess the contractility and electrophysiology of the cardiac tissues. For imaging, tissues were incubated at 37 °C and 5% CO_2 for 90 min in Tyrode's solution containing 5 μM calcium indicator Cal 520 AM (21130, AAT Bioquest) and 0.025% Pluronic F127 (P2443, Sigma Aldrich). Tissues were then transferred into a 50 × 35 mm imaging dish (23000-5035, Kimax) and incubated in Tyrode's solution for 30 min at 37 °C for equilibration. Finally, the imaging dish was transferred onto a custom heated stage maintained at 37 ± 1 °C throughout the experiment. High-speed imaging of up to 100 frames per second was performed using a scientific CMOS camera (Prime 95B, Photometrics) mounted on an epifluorescent stereomicroscope (MVX10, Olympus) with a Sola Light Engine (Lumencor) and a GFP filter cube. Excitation–contraction decouplers were not used when imaging the entire tissue at 1.25× magnification because there was minimal motion artifact. Custom Python and MATLAB scripts built upon published methods were used to create isochrone maps, calcium traces, quantification of conduction velocity, and calculation of calcium trace metrics.[30] A dynamic tissue mask was generated from each frame, and the average pixel intensity of the tissue strip was calculated at each frame and plotted over time. Each data point was then normalized to peak intensity frame at diastole (F/F$_0$ -1). In addition, Image J analysis software was used for calcium signal region-of-interest (ROI) analysis based on the criteria that (a) there was minimal motion artifact in that ROI and (b) that the entire ROI contained actively contracting cells.

Pharmacological studies

2D Monolayer studies

The 2D cardiomyocyte monolayer pharmacological studies were conducted using hiPSC-CMs cultured on glass coverslips. Briefly, hiPSC-CMs (iCell Cardiomyocytes,[2] Fujifilm Cellular Dynamics) were thawed according to the manufacturer's instructions and plated at a density of 30 000 cells/well in 96-well plates (655090, Greiner Bio-One) that had been pre-coated with fibronectin (50 μg/ml) for 3 h at 37 °C. Cells were cultured for 48 h in plating media and switched to maintenance media (R1151, Fujifilm Cellular Dynamics). Maintenance media was changed every other day and 24 h prior to the day of the experiment. Cells were assayed 14-days after plating. The hiPSC-CMs were incubated with Codex ACTOne Calcium Dye (Codex Biosolutions, Rockville, MD) according to the manufacturer's instructions for 1 h at 37 °C, 5% CO2. An FDSS/μCell imaging platform heated internally to 37 °C (Hamamatsu Ltd., Hamamatsu, Japan) was used as the fluorescence plate reader, with excitation wavelength of 470 nm and the emitted light passed through a 540 nm bandpass filter. A CCD camera simultaneously collected Ca^{2+} transient signals from all 96-wells, at a frame sampling rate of 16 Hz for 1 min. After loading the dye, a baseline recording was taken. Subsequently, isoproterenol was added from compound stocks in DMSO such that the final concentration of DMSO was 0.1%. All compound concentrations were applied in triplicate (n = 3 wells/concentration) for each batch of iCells tested (total of three separate iCell batches). Time-matched vehicle wells (0.1% DMSO) were assayed alongside to correct for any time- and/or vehicle-dependent effects on measured parameters. Data of each well were normalized to baseline of that well, then normalized to time-matched 0.1% DMSO control, and then averaged. Results are reported as mean (n = 9 wells per concentration).

3D cardiac tissue studies

The pharmacological studies on the FRESH[TM] printed 3D cardiac tissues were performed after 14 days in culture in Tyrode's solution using the calcium imaging system already described. Tissues were allowed to equilibrate in the custom heated stage maintained at 37 ± 1 °C and then imaged at baseline and following exposure to isoproterenol (I6504, Sigma Aldrich). For saturation experiments, a single dose of drug was used. For dose response studies, each dosage of drug was added sequentially from lowest to highest and each dosage addition was followed by a 10 min incubation period prior to imaging. Each dosage of drug was prepared and warmed to 37 °C immediately prior to its addition to the tissue to ensure no degradation of drug over time. All drug concentrations were prepared from a 10 mM stock solution dissolved in DMSO and Tyrode's solution and were further

serially diluted in Tyrode's solution. Tissues were only included for measured calcium amplitude if they demonstrated significant change in beat frequency response to isoproterenol.

Immunofluorescence staining, imaging, and analysis

Cardiac tissue strips were fixed and permeabilized overnight at 4 °C in 3.7% formaldehyde (252549, Sigma Aldrich) and 0.25% Triton X-100 (T9284, Sigma Aldrich) in 1× phosphate buffered saline (PBS). The tissues were washed and blocked in 4% fetal bovine serum, 0.1% Triton X-100, 50 mM glycine, 1 mM calcium, and 1 mM magnesium in 1X PBS overnight at 4 °C. The tissues were then washed and stained with 1:100 dilution of mouse anti-sarcomeric α-actinin primary antibody (A7811, Sigma-Aldrich) and 1:100 rabbit anti-CD31 (AB32457, Abcam) for 48 h at 4 °C. Following primary antibody staining, tissues were washed and stained for 48 h at 4 °C with a 1:100 dilution of goat anti-mouse secondary antibody conjugated to Alexa-Fluor 488 (A28175, Life Technologies), goat anti-rabbit secondary antibody conjugated to Alexa-Fluor 555 (A21428, Life Technologies) at a 1:100 dilution, To-Pro3 at a 1:400 dilution and phalloidin conjugated to Alexa-Fluor 633 (A22284, Life Technologies) at a 1:50 dilution. Tissues were then washed of excess secondary antibodies. Confocal Z-stacks of tissue strips were acquired using 25× and 63× oil-immersion objective lenses on a Zeiss LSM 980 with Airy Scan. Data were exported to Image J and Imaris 3D segmentation software for processing and visualization. Tissue cell density was calculated in Imaris from the total number of segmented nuclei within the volume of a tissue outlined by actin cytoskeleton staining.

Statistical analysis

GraphPad Prism 9 was used for all statistical analysis. A one-tailed, paired T-test was used to evaluate the saturated response of tissue strips to isoproterenol ($\alpha = 0.05$). The non-linear regression fit function with four parameters was used to create dose response curves.

SUPPLEMENTARY MATERIALS

See the supplementary material for additional details on manufacturing reproducibility of the FRESH[TM] 3D bioprinting platform described here, specifically to generate geometrically and functionally reproducible cardiac tissues.

AUTHOR DECLARATIONS
Conflict of Interest

The authors have no conflicts to disclose.

Ethics Approval

Ethics approval is not required.

Author Contributions

Samuel Finkel: Conceptualization (equal); Data curation (lead); Formal analysis (lead); Investigation (lead); Methodology (lead); Project administration (lead); Software (equal); Visualization (lead); Writing – original draft (equal); Writing – review & editing (equal). **Armando Lagrutta:** Funding acquisition (equal); Methodology (supporting); Supervision (equal); Writing – review & editing (supporting). **Adam Feinberg:** Conceptualization (equal); Data curation (equal); Funding acquisition (equal); Supervision (equal); Writing – review & editing (equal). **Andrew Lee:** Conceptualization (lead); Data curation (lead); Formal analysis (lead); Funding acquisition (equal); Investigation (supporting); Methodology (equal); Project administration (equal); Supervision (lead); Visualization (lead); Writing – original draft (lead); Writing – review & editing (lead). **Shannon Sweet:** Investigation (equal); Methodology (equal). **Tyler Locke:** Investigation (equal); Methodology (equal). **Sydney Smith:** Software (lead). **Zhefan Wang:** Investigation (supporting); Methodology (supporting). **Christopher Sandini:** Resources (equal); Supervision (supporting). **John Imredy:** Conceptualization (equal); Funding acquisition (equal); Methodology (supporting); Supervision (equal); Writing – review & editing (supporting). **Yufang He:** Conceptualization (equal); Funding acquisition (equal); Methodology (equal); Supervision (equal); Writing – review & editing (equal). **Marc Durante:** Funding acquisition (equal); Resources (supporting); Supervision (supporting).

DATA AVAILABILITY

The data that support the findings of this study are available within the article and its supplementary material.

REFERENCES

[1]World Health Organization, *World Health Statistics 2019: Monitoring Health for the SDGs, Sustainable Development Goals* (World Health Organization, 2019).
[2]X. Rossello, S. J. Pocock, and D. G. Julian, "Long-term use of cardiovascular drugs: Challenges for research and for patient care," J. Am. College Cardiol. **66**, 1273–1285 (2015).
[3]M. McClellan, N. Brown, R. M. Califf, and J. J. Warner, "Call to action: Urgent challenges in cardiovascular disease: A presidential advisory from the American Heart Association," Circulation **139**, e44–e54 (2019).
[4]I. Khanna, "Drug discovery in pharmaceutical industry: Productivity challenges and trends," Drug Discovery Today **17**, 1088–1102 (2012).
[5]G. A. Figtree *et al.*, "A call to action for new global approaches to cardiovascular disease drug solutions," Circulation **144**, 159–169 (2021).
[6]C. B. Fordyce *et al.*, "Cardiovascular drug development," J. Am. College Cardiol. **65**, 1567–1582 (2015).
[7]G. Gromo, J. Mann, and J. D. Fitzgerald, "Cardiovascular drug discovery: A perspective from a research-based pharmaceutical company," Cold Spring Harbor Perspect. Med. **4**, a014092 (2014).
[8]C. Riehle and J. Bauersachs, "Small animal models of heart failure," Cardiovasc. Res. **115**, 1838–1849 (2019).
[9]L. O. Lerman *et al.*, "Animal models of hypertension: A scientific statement from the American Heart Association," Hypertension **73**, e87–e120 (2019).
[10]R. Paul, "FDA modernization Act 2.0," in 117th Cong., S. 5002 (2022).
[11]H. Tani and S. Tohyama, "Human engineered heart tissue models for disease modeling and drug discovery," Front. Cell Dev. Biol. **10**, 855763 (2022).
[12]P. W. Burridge *et al.*, "Chemically defined generation of human cardiomyocytes," Nat. Methods **11**, 855–860 (2014).
[13]C. W. Scott *et al.*, "An impedance-based cellular assay using human iPSC-Derived cardiomyocytes to quantify modulators of cardiac contractility," Toxicol. Sci. **142**, 331–338 (2014).

[14]K. Blinova *et al.*, "Comprehensive translational assessment of human-induced pluripotent stem cell derived cardiomyocytes for evaluating drug-induced arrhythmias," Toxicol. Sci. **155**, 234–247 (2017).

[15]S. D. Burnett, A. D. Blanchette, W. A. Chiu, and I. Rusyn, "Human induced pluripotent stem cell (iPSC)-derived cardiomyocytes as an *in vitro* model in toxicology: Strengths and weaknesses for hazard identification and risk characterization," Expert. Opin. Drug Metab. Toxicol. **17**, 887–902 (2021).

[16]S. Cho, D. E. Discher, K. W. Leong, G. Vunjak-Novakovic, and J. C. Wu, "Challenges and opportunities for the next generation of cardiovascular tissue engineering," Nat. Methods **19**, 1064–1071 (2022).

[17]D. Thomas, S. Choi, C. Alamana, K. K. Parker, and J. C. Wu, "Cellular and engineered organoids for cardiovascular models," Circ. Res. **130**, 1780–1802 (2022).

[18]P. Lee *et al.*, "Simultaneous voltage and calcium mapping of genetically purified human induced pluripotent stem cell-derived cardiac myocyte monolayers," Circ. Res. **110**, 1556–1563 (2012).

[19]N. T. Elliott and F. Yuan, "A review of three-dimensional *in vitro* tissue models for drug discovery and transport studies," J. Pharm. Sci. **100**, 59–74 (2011).

[20]H. Kim, R. D. Kamm, G. Vunjak-Novakovic, and J. C. Wu, "Progress in multi-cellular human cardiac organoids for clinical applications," Cell Stem Cell **29**, 503–514 (2022).

[21]J. H. Ahrens *et al.*, "Programming cellular alignment in engineered cardiac tissue via bioprinting anisotropic organ building blocks," Adv. Mater. **34**, 2200217 (2022).

[22]H. Chang *et al.*, "Recreating the heart's helical structure-function relationship with focused rotary jet spinning," Science **377**, 180–185 (2022).

[23]C. E. Rupert, H. H. Chang, and K. L. K. Coulombe, "Hypertrophy changes 3D shape of hiPSC-cardiomyocytes: Implications for cellular maturation in regenerative medicine," Cell. Mol. Bioeng. **10**, 54–62 (2017).

[24]D. B. Kolesky, K. A. Homan, M. A. Skylar-Scott, and J. A. Lewis, "Three-dimensional bioprinting of thick vascularized tissues," Proc. Natl. Acad. Sci. U. S. A. **113**, 3179–3184 (2016).

[25]I. Goldfracht *et al.*, "Generating ring-shaped engineered heart tissues from ventricular and atrial human pluripotent stem cell-derived cardiomyocytes," Nat. Commun. **11**, 75 (2020).

[26]B. Liau, N. Christoforou, K. W. Leong, and N. Bursac, "Pluripotent stem cell-derived cardiac tissue patch with advanced structure and function," Biomaterials **32**, 9180–9187 (2011).

[27]R. A. Li *et al.*, "Bioengineering an electro-mechanically functional miniature ventricular heart chamber from human pluripotent stem cells," Biomaterials **163**, 116–127 (2018).

[28]W. Keung *et al.*, "Human cardiac ventricular-like organoid chambers and tissue strips from pluripotent stem cells as a two-tiered assay for inotropic responses," Clin. Pharmacol. Ther. **106**, 402–414 (2019).

[29]J. M. Bliley *et al.*, "Dynamic loading of human engineered heart tissue enhances contractile function and drives desmosome-linked disease phenotype," bioRxiv (2020).

[30]A. Lee *et al.*, "3D bioprinting of collagen to rebuild components of the human heart," Science **365**, 482–487 (2019).

[31]T. J. Hinton *et al.*, "Three-dimensional printing of complex biological structures by freeform reversible embedding of suspended hydrogels," Sci. Adv. **1**, e1500758 (2015).

[32]S. M. Ravenscroft, A. Pointon, A. W. Williams, M. J. Cross, and J. E. Sidaway, "Cardiac non-myocyte cells show enhanced pharmacological function suggestive of contractile maturity in stem cell derived cardiomyocyte microtissues," Toxicol. Sci. **152**, 99–112 (2016).

[33]J. W. Tashman, D. J. Shiwarski, and A. W. Feinberg, "A high performance open-source syringe extruder optimized for extrusion and retraction during FRESH^{TM} 3D bioprinting," HardwareX **9**, e00170 (2021).

[34]M. E. Kupfer *et al.*, "*In situ* expansion, differentiation, and electromechanical coupling of human cardiac muscle in a 3D bioprinted, chambered organoid," Circ. Res. **127**, 207–224 (2020).

[35]J. Liu *et al.*, "Rapid 3D bioprinting of *in vitro* cardiac tissue models using human embryonic stem cell-derived cardiomyocytes," Bioprinting **13**, e00040 (2019).

[36]M. Mollova *et al.*, "Cardiomyocyte proliferation contributes to heart growth in young humans," Proc. Natl. Acad. Sci. U. S. A. **110**, 1446–1451 (2013).

[37]K. Ronaldson-Bouchard *et al.*, "Advanced maturation of human cardiac tissue grown from pluripotent stem cells," Nature **556**, 239–243 (2018).

[38]S. B. Bremner, K. S. Gaffney, N. J. Sniadecki, and D. L. Mack, "A change of heart: Human cardiac tissue engineering as a platform for drug development," Curr. Cardiol. Rep. **24**, 473–486 (2022).

[39]A. Hansen *et al.*, "Development of a drug screening platform based on engineered heart tissue," Circ. Res. **107**, 35–44 (2010).

[40]M. Tiburcy *et al.*, "Defined engineered human myocardium with advanced maturation for applications in heart failure modelling and repair," Circulation **135**(19), 1832–1847 (2017).

[41]Y. Zhao *et al.*, "A platform for generation of chamber-specific cardiac tissues and disease modeling," Cell **176**, 913–927 (2019).

[42]M. H. Draper and M. Mya-Tu, "A comparison of the conduction velocity in cardiac tissues of various mammals," Exp. Physiol. **44**, 91–109 (1959).

[43]A. F. M. Moorman, F. de Jong, M. M. F. J. Denyn, and W. H. Lamers, "Development of the cardiac conduction system," Circ. Res. **82**, 629–644 (1998).

[44]W.-H. Zimmermann *et al.*, "Tissue engineering of a differentiated cardiac muscle construct," Circ. Res. **90**, 223–230 (2002).

[45]M. Radisic *et al.*, "Oxygen gradients correlate with cell density and cell viability in engineered cardiac tissue," Biotechnol. Bioeng. **93**, 332–343 (2006).

[46]C. Jackman, H. Li, and N. Bursac, "Long-term contractile activity and thyroid hormone supplementation produce engineered rat myocardium with adult-like structure and function," Acta Biomater. **78**, 98–110 (2018).

[47]S. Shen *et al.*, "Physiological calcium combined with electrical pacing accelerates maturation of human engineered heart tissue," Stem Cell Rep. **17**, 2037–2049 (2022).

[48]M. Dostanic *et al.*, "A miniaturized EHT platform for accurate measurements of tissue contractile properties," J. Microelectromech. Syst. **29**, 881–887 (2020).

[49]A. Eder, I. Vollert, A. Hansen, and T. Eschenhagen, "Human engineered heart tissue as a model system for drug testing," Adv. Drug Delivery Rev. **96**, 214–224 (2016).

[50]E. Giacomelli *et al.*, "Human-iPSC-derived cardiac stromal cells enhance maturation in 3D cardiac microtissues and reveal non-cardiomyocyte contributions to heart disease," Cell Stem Cell **26**, 862–879 (2020).

[51]J. Davis *et al.*, "*In vitro* model of ischemic heart failure using human induced pluripotent stem cell-derived cardiomyocytes," JCI Insight **6**, e134368 (2021).

[52]E. Tzatzalos, O. J. Abilez, P. Shukla, and J. C. Wu, "Engineered heart tissues and induced pluripotent stem cells: Macro- and microstructures for disease modeling, drug screening, and translational studies," Adv. Drug Delivery Rev. **96**, 234–244 (2016).

[53]M. Endoh, "Force–frequency relationship in intact mammalian ventricular myocardium: Physiological and pathophysiological relevance," Eur. J. Pharmacol. **500**, 73–86 (2004).

[54]A. F. G. Godier-Furnémont *et al.*, "Physiologic force-frequency response in engineered heart muscle by electromechanical stimulation," Biomaterials **60**, 82–91 (2015).

[55]B. Pieske *et al.*, "Diminished post-rest potentiation of contractile force in human dilated cardiomyopathy. Functional evidence for alterations in intracellular Ca^{2+} handling," J. Clin. Invest. **98**, 764–776 (1996).

[56]N. T. Feric and M. Radisic, "Maturing human pluripotent stem cell-derived cardiomyocytes in human engineered cardiac tissues," Adv. Drug Delivery Rev. **96**, 110–134 (2016).

[57]G. A. Ramirez-Correa and A. M. Murphy, "Is phospholamban or troponin I the 'prima donna' in β-adrenergic induced lusitropy?," Circ. Res. **101**, 326–327 (2007).

[58]S. Weiss, S. Oz, A. Benmocha, and N. Dascal, "Regulation of cardiac L-type Ca^{2+} channel CaV1.2 via the β-adrenergic-cAMP-protein kinase a pathway: Old dogmas, advances, and new uncertainties," Circ. Res. **113**, 617–631 (2013).

[59]L. Guo *et al.*, "Estimating the risk of drug-induced proarrhythmia using human induced pluripotent stem cell-derived cardiomyocytes," Toxicol. Sci. **123**, 281–289 (2011).

[60]K. Harris *et al.*, "Comparison of electrophysiological data from human-induced pluripotent stem cell-derived cardiomyocytes to functional preclinical safety assays," Toxicol. Sci. **134**, 412–426 (2013).

[61]M. C. S. C. Vermeer *et al.*, "Gain-of-function mutation in ubiquitin ligase KLHL24 causes desmin degradation and dilatation in hiPSC-derived engineered heart tissues," J. Clin. Invest. **131**, e140615 (2021).

[62]K. Ronaldson-Bouchard, "Engineering of human cardiac muscle electromechanically matured to an adult-like phenotype," Nat. Protocols **14**(10), 2781–2817 (2019).

[63]C. A. Lopez et al., "Physiological and pharmacological stimulation for *in vitro* maturation of substrate metabolism in human induced pluripotent stem cell-derived cardiomyocytes," Sci. Rep. **11**, 7802 (2021).

[64]X. Yang et al., "Fatty acids enhance the maturation of cardiomyocytes derived from human pluripotent stem cells," Stem Cell Rep. **13**, 657–668 (2019).

[65]Y. Guo and W. T. Pu, "Cardiomyocyte maturation: New phase in development," Circ. Res. **126**, 1086–1106 (2020).

[66]A. Yoshida et al., "Development of appropriate fatty acid formulations to raise the contractility of constructed myocardial tissues," Regener. Ther. **21**, 413–423 (2022).

[67]G. Galati et al., "Histological and histometric characterization of myocardial fibrosis in end-stage hypertrophic cardiomyopathy: A clinical-pathological study of 30 explanted hearts," Circulation **9**, e003090 (2016).